Geophysical Research Letters

REPLY

10.1029/2024GL111599

Reply to Comment by Chang on "Anticyclonic Suppression of the North Pacific Transient Eddy Activity in Midwinter"

Satoru Okajima[1], **Hisashi Nakamura**[1], **and Yohai Kaspi**[2]

[1]Research Center for Advanced Science and Technology, The University of Tokyo, Tokyo, Japan, [2]Department of Earth and Planetary Sciences, Weizmann Institute of Science, Rehovot, Israel

Key Points:

- The error in attributing eddy statistics to cyclones and anticyclones is significantly smaller than that presented by Chang (2024, https://doi.org/10.1029/2024gl110011)
- The arguments of Chang (2024, https://doi.org/10.1029/2024gl110011) are based on the unrealistic assumptions of monopolar vorticity and an atypical background flow
- The curvature-based evaluation of cyclonic and anticyclonic contributions is a practical, beneficial method for realistic flow fields

Correspondence to:

S. Okajima,
okajima@atmos.rcast.u-tokyo.ac.jp

Citation:

Okajima, S., Nakamura, H., & Kaspi, Y. (2024). Reply to comment by Chang on "anticyclonic suppression of the North Pacific transient eddy activity in midwinter". *Geophysical Research Letters*, *51*, e2024GL111599. https://doi.org/10.1029/2024GL111599

Received 9 AUG 2024
Accepted 11 SEP 2024

Abstract Chang (2024, https://doi.org/10.1029/2024gl110011) challenged the methodology proposed recently by Okajima et al. for evaluating cyclonic and anticyclonic contributions to Eulerian eddy statistics and atmospheric energetics based on the local flow curvature. He argued that using the local wind curvature to separate energetic contributions from cyclones and anticyclones is not physically meaningful. Here we argue that his claims are based on an unrealistic assumption of monopolar relative vorticity in an entire storm-track domain and a meridionally uniform zonal background flow atypical to midlatitudes. We also demonstrate that the error in attributing eddy statistics to cyclones and anticyclones is significantly smaller than his estimation. Rather, we further demonstrate that the curvature-based methodology effectively eliminates the shear influence to identify cyclonic and anticyclonic regions, which is dismissed in his argument. We conclude that the curvature-based methodology is beneficial in evaluating distinct cyclonic and anticyclonic contributions to atmospheric energetics in realistic conditions.

Plain Language Summary Chang (2024, https://doi.org/10.1029/2024gl110011) raised a question about the effectiveness of the recent method by Okajima et al. for evaluating cyclonic and anticyclonic contributions separately to eddy statistics based on the local flow curvature. He brings idealized cases to claim that the method by Okajima et al. is not physically meaningful. Here we show that Chang's arguments rely on an unrealistic assumption that an entire storm-track region contains only one or two isolated cyclonic vorticity patches placed within horizontally uniform westerlies, which are atypical of midlatitudes. We also reveal that the error in attributing eddy statistics to cyclones and anticyclones is much smaller than Chang's result. The curvature-based method effectively removes the influence of shear vorticity to determine cyclonic and anticyclonic regions, which is overlooked in his argument. We conclude that our curvature-based method is useful for evaluating the separate contributions of cyclones and anticyclones to atmospheric energetics in realistic conditions in midlatitudes.

Eulerian eddy statistics based on high-pass-filtered atmospheric variables are widely used to study storm-track activity with their easy applicability to reanalysis data sets (Chang et al., 2002; Wallace et al., 1988) and climate model outputs (Eyring et al., 2021), and their suitability for quantitative dynamical diagnostics (Hoskins et al., 1983; Orlanski and Katzfey, 1991). Nevertheless, Eulerian eddy statistics such as eddy kinetic energy (EKE) are incapable of separating contributions between cyclones and anticyclones, despite the differences between the spatial distributions of Eulerian eddy statistics and Lagrangian cyclone tracks (e.g., Shaw et al., 2016), and between their seasonality (Okajima et al., 2022, 2023). Wallace et al. (1988) pointed out that Eulerian eddy statistics are not necessarily dominated by cyclones. This incapability has limited our understanding of storm-track dynamics and related eddy-mean flow interactions.

As an attempt to resolve this issue, Okajima, Nakamura, and Kaspi (2024; hereafter ONK24) evaluated cyclonic and anticyclonic contributions separately to Eulerian eddy statistics and atmospheric energetics based on instantaneous identification of cyclonic and anticyclonic regions according to the local curvature of the flow, expanding a practical, ad hoc method developed by Okajima et al. (2021). The curvature of the flow effectively eliminates the influence of shear vorticity associated with strong midlatitude jets in storm-track regions, to determine cyclonically and anticyclonically rotating regions embedded in these jets. The curvature also has an advantage in its independence of scalar wind speed and straightforward physical meaning, in that its reciprocal is a curvature radius of the flow.

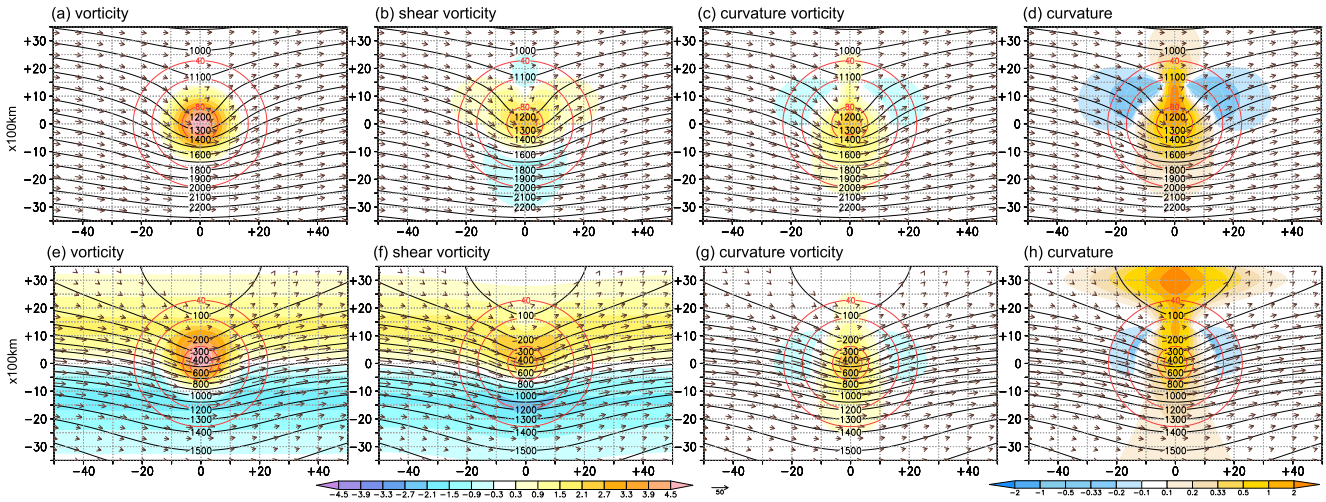

Figure 1. Simple cases. (a–d) Relative vorticity (a; 10^{-5} s^{-1}; colored as indicated), shear vorticity (b; 10^{-5} s^{-1}), curvature vorticity (c; 10^{-5} s^{-1}), and curvature (d; 10^{-6} m^{-1}) in the case where an isolated cyclonic eddy is superimposed onto horizontally uniform background westerlies (Case 1). Arrows denote horizontal winds (m s^{-1}). Black contours indicate geopotential height (m). Red contours indicate kinetic energy associated with the eddy flow defined as wind fields associated with the vortex in a resting background state (m^2 s^{-2}). Panels (e–h) same as in (a–d), respectively, but for the corresponding fields in the case where the cyclonic eddy is superimposed on a meridionally-confined westerly jet (Case 2).

Chang (2024) raised a question about the effectiveness of the methodology proposed by ONK24. Using idealized examples in which a cyclonic vortex with an isolated positive relative vorticity maximum embedded in constant horizontally uniform westerlies, he argued that two large regions of negative (anticyclonic) curvature are observed east and west of the isolated cyclonic vortex, although there is only a cyclone with no anticyclones in the domain. He also showed that the fraction of EKE "misattributed" as contributions from regions of anticyclonic curvature depends on the speed of the background flow when we set a non-zero curvature threshold as in ONK24. He claimed that the attribution of a substantial fraction of EKE to anticyclones in his examples is erroneous and further argued that using the curvature of the local wind to separate energetic contributions from cyclones and anticyclones is not physically meaningful.

First, we show that his results rely on specific configurations of the flows. Figures 1a–1d depict an idealized case where an isolated cyclonic eddy is superimposed on horizontally uniform westerlies (Case 1), which corresponds to Chang's first case. In Case 1, we assume a geopotential height field Z in a 20,000 km-wide square domain on an f-plane as

$$Z = \frac{-y + L_y/2}{L_y} Z_B + \int_{L_y/2}^{y} -\frac{f_0}{g} U_0 \exp\left(-\frac{y^2}{2U_y^2}\right) dy + \frac{f_0}{g} \nabla^{-2} \left\{ E_0 \exp\left(-\frac{y^2}{2E_y^2}\right) \exp\left(-\frac{x^2}{2E_x^2}\right) \right\}, \quad (1)$$

where $Z_B = 0$ m denotes the background gradient of geopotential height, $U_0 = 20$ m s^{-1} the intensity of the westerly flow, $U_y = 10^{10}$ km the width of the westerly flow, $E_0 = 5.0 \times 10^{-5}$ s^{-1} the amplitude of eddies in vorticity, $E_x = 700$ km and $E_y = 700$ km the zonal and meridional scales of eddies, respectively, L_y(=20,000 km) the meridional size of the domain, and f_0 the Coriolis parameter (fixed to the value at 45°N). Although relative vorticity is axisymmetric (Figure 1a), curvature vorticity is non-axisymmetric (Figure 1c) to cancel shear vorticity induced by the superposition of the eddy on the background flow (Figure 1b). As pointed out by Chang (2024), the curvature field is correspondingly distorted (Figure 1d), which is indeed meaningful in that the anticyclonic curvature (vorticity) regions indicate local supergeostrophy. The meridionally uniform background flow is, however, atypical in storm-track regions, which are characterized by sharp and strong extratropical jets (e.g., Spensberger et al., 2017), as in our Case 2.

Figures 1e–1h depict Case 2, where a more realistic, meridionally confined jet is prescribed as a background of the cyclonic vortex. In Case 2, we set $Z_B = 800$ m, $U_0 = 35$ m s^{-1}, and $U_y = 1{,}300$ km in Equation 1 with the other parameters identical to those in Case 1. In this case, determining a cyclonic region based on the relative vorticity

field (Figure 1e) is more difficult compared with Case 1 (Figure 1a), because of shear vorticity (Figure 1f) associated with the jet. Curvature vorticity (Figure 1g) effectively eliminates the influence of shear vorticity if compared with relative vorticity (Figure 1e). Indeed, effective removal of the influence of the lateral shear of westerly jets is an essential advantage of our methodology (ONK24), which is dismissed in Chang's argument. Although there are still two regions of anticyclonic curvature west and east of the vortex (Figure 1h), they are much less distinct compared with those in Case 1 (Figure 1d). Contributions of cyclonic regions at latitudes far away from the vortex and jet to Eulerian eddy statistics are also limited because the corresponding curvature vorticity is weak (Figure 1g). Moreover, we can set a non-zero threshold for determining cyclonic and anticyclonic domains (ONK24) to verify the robustness of the results against the arbitrariness in cutting domains of strong winds in cyclone-anticyclone transition zones into half.

Chang (2024) pointed out that the dependence of the fraction of cyclone-related EKE attributed as contributions of anticyclonic regions upon the speed of the background flow. We have found, however, that it is also sensitive to specific configurations of the flows. Figure 2a shows the fraction of EKE attributed to cyclonic and anticyclonic regions in Cases 1 and 2 based on a curvature threshold of $\pm 0.33 \times 10^{-6}$ m^{-1}. The sum of the fraction of cyclonic and anticyclonic EKE decreases with background wind speed, probably because the effect of strong background winds acts to reduce the curvature of the flow. Consistent with Chang (2024), the fraction of EKE attributed to anticyclonic regions is maximized under a moderate background wind speed ($\sim$15 m s^{-1}) in Case 1 (blue dashed line in Figure 2a). Nevertheless, the fraction of anticyclonic EKE is $\sim$10% at maximum, which is much smaller than the value ($\sim$30%) presented by Chang (2024). Furthermore, in the more realistic jet-like case (Case 2; solid lines in Figure 2a), the fraction of anticyclonic EKE is nearly zero regardless of the background jet intensity. Additionally, under moderate and strong jet intensities, the fraction of cyclonic EKE is systematically higher than that in Case 1. We therefore consider that Chang's argument that the separation based on the flow curvature is erroneous is misleading as it is based on the atypical cases. Note that a non-zero curvature threshold as in ONK21 works better than a threshold of zero curvature (Figure 2b) for these two cases.

Furthermore, the assumption of monopolar relative vorticity contained in the entire domain in Chang's examples is also unrealistic. His idealized cases contain only one or two isolated cyclonic relative vorticity patches in a square domain, which is 10,000 km wide. When averaged over the entire globe, relative vorticity should be zero due to the cancellation of divergence/convergence and its fluxes (e.g., Holton, 2004). This suggests that there must be regions of both positive and negative relative vorticity in a relatively wide domain, such as the North Pacific and Atlantic storm-track regions. To see if this is indeed the case, Figure 2c shows the distribution of the ratio of instantaneous area-averaged vorticity only over the grid points of cyclonic vorticity to the corresponding average of anticyclonic vorticity, within the Nort Pacific. The length and width of the domain focused here are $\sim$5,000 km. The ratio is distributed approximately around unity and very unlikely to be larger (smaller) than 1.75 (0.5). Chang (2024) argued that his assumption of monopolar cyclonic vorticity reflects the observation that cyclonic vortices are observed much more frequently than anticyclonic vortices (Hoskins & Hodges, 2002). This may be consistent with a positively skewed distribution of the ratio between the numbers of grid points of cyclonic and anticyclonic vorticity, whose mean is substantially smaller than unity (green line in Figure 2c). This skewed distribution is indicative of the statistically more coherent structure of cyclonic vortices, which is likely favorable for their identification by automated algorithms. Nevertheless, the frequency distribution in Figure 2c corroborates that Chang's argument based on monopolar cyclonic vorticity is unrealistic and thus unjustified, given that, in his examples, area-averaged anticyclonic vorticity is zero and the ratio between area-averaged cyclonic and anticyclonic vorticity is infinity. If the condition of near-zero area-averaged relative vorticity in the domain is to be met, we should have anticyclonic regions everywhere out of the isolated cyclonic vortex, where the attribution of EKE partly to anticyclones is reasonable. These results also substantiate that Case 2 (Figures 1e–1h) is much more realistic than Case 1 (Figures 1a–1d).

The methodology by ONK24 aims to obtain long-term climatological means of Eulerian eddy statistics and atmospheric energetics. We do not claim that our methodology is always precisely accurate, and thus we regard it as "practical, ad hoc." Although it may be possible to pick up unrealistic, atypical cases like an isolated monopolar cyclone in horizontally uniform westerlies (Chang, 2024; Figures 1a–1d), the overall value of our curvature-based framework, which is effective in realistic conditions, cannot be degraded.

Chang's claim that the separation of cyclonic and anticyclonic contributions based on flow curvature is physically meaningless assumes that we can obtain a priori knowledge about which vorticity anomalies are dynamical and

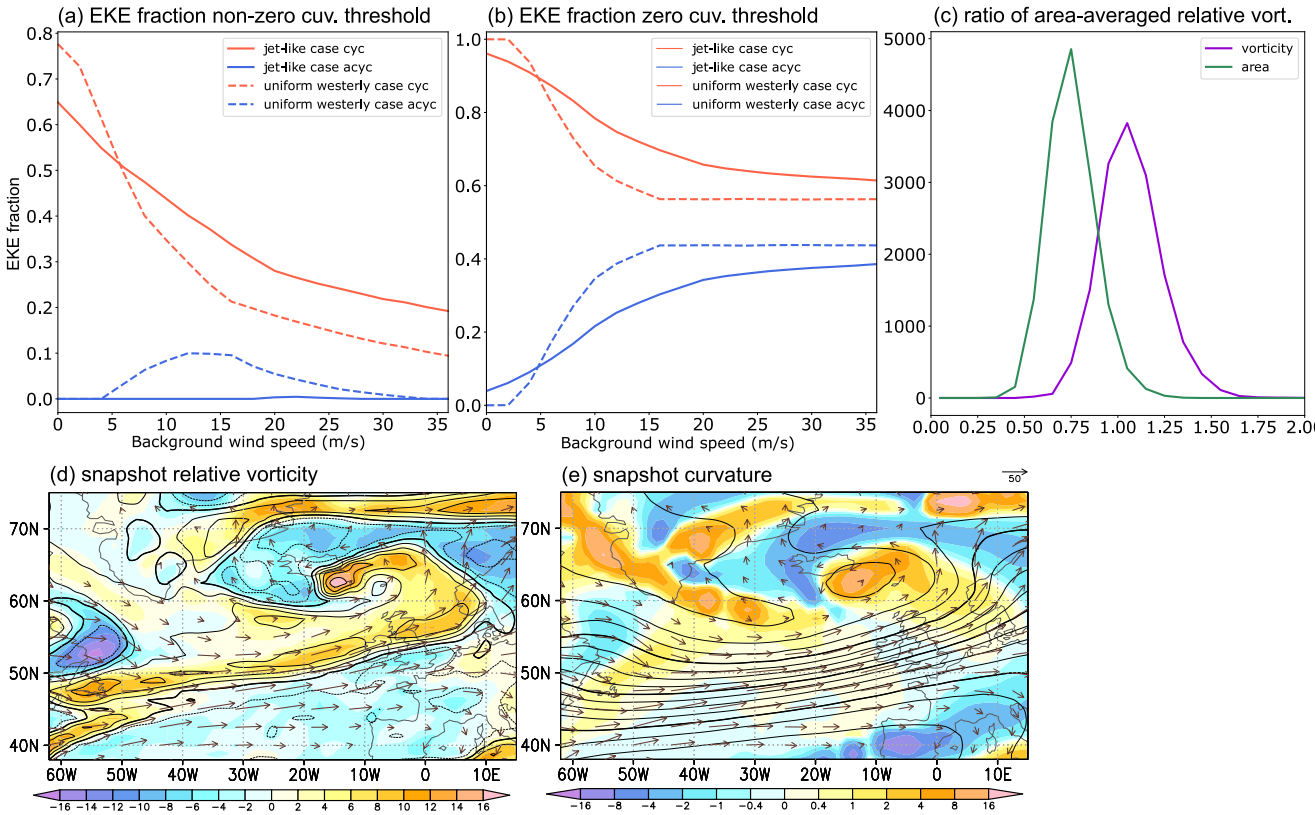

Figure 2. (a) Fraction of eddy kinetic energy (EKE) within cyclonic (red lines) and anticyclonic (blue lines) regions as a function of the background flow or jet strength (m s^{-1}; U_0) based on a curvature threshold of $\pm 0.33 \times 10^{-6}$ m^{-1} (as in Chang (2024) and ONK24). Dashed and solid lines denote results based on Cases 1 and 2, respectively. EKE is averaged horizontally within the domain shown in Figure 1. Note that the vortex has a maximum wind speed of about 15 m s^{-1}. Panel (b) same as in (a), but for a curvature threshold of zero. (c) Frequency distribution of the ratio of relative vorticity averaged only over grid points of positive values to that averaged only for negative values (purple) within (155°E−155°W, 15°N−60°N) in January and February for the period of 1959–2022 (the total sample size is 15,168). Values larger than unity mean that positive vorticity dominates negative vorticity. Green line denotes the corresponding frequency distribution of the ratio between the numbers of grid points of positive and negative relative vorticity in the domain. (d) Eight-day high-pass-filtered 300-hPa relative vorticity (colors as indicated; 10^{-5} s^{-1}) at 00z11Jan1993 over the North Atlantic (Odell et al., 2013). Black contours indicate unfiltered 300-hPa relative vorticity (every 4×10^{-5} s^{-1}; thick for zero contours). Arrows signify unfiltered 300-hPa horizontal winds (m s^{-1}). Panel (e) same as in (d) but for local curvature of unfiltered horizontal winds (colors; 10^{-6} m^{-1}) and unfiltered 300-hPa geopotential height (black contours; every 100 m and thick for every 400 m). All variables shown are from the JRA-55 reanalysis (Harada et al., 2016; Kobayashi et al., 2015).

thus physically meaningful. In the real atmosphere, however, we usually observe both positive and negative relative vorticity, associated with its shear and curvature components, in the basin-scale storm-track regions. Unlike in his argument, it is therefore impossible to obtain a priori knowledge about which portion of a given vorticity field is associated with a cyclonic or anticyclonic vortex and which is a dynamically more active system. Rather, it is a purpose of the ad hoc, practical curvature-based methodology by ONK24 to identify cyclonic and anticyclonic vortices embedded in westerly jets, which immediately leads to the separation of Eulerian eddy statistics widely used in storm-track studies into cyclonic and anticyclonic contributions. Calculating the local curvature of the flow is also beneficial since it can be a source of cyclone/anticyclone asymmetry through the difference in the role of centripetal acceleration.

The difficulties in determining which portion of a given upper-level vorticity (or potential vorticity) anomaly field is associated with a cyclonic or anticyclonic vortex can be seen in an actual case (Figures 2d and 2e). Upper-level vorticity is influenced strongly by shear vorticity of westerly jets (Okajima et al., 2021; Figures 2d and 2e), which is overlooked by Chang (2024). Additionally, a cyclone (or cyclonic vortex) is unlikely to consist only of a simple circular-shaped, isolated anomaly of positive vorticity. Rather, positive anomalies of vorticity are confined into a much smaller region around the cyclone center (Figure 2d) compared with the trough or cut-off low represented by geopotential height and curvature (Figure 2e), which is likely related to precipitation associated with the cyclone.

Distributions of fluctuating winds and other variables associated with baroclinic eddies can be viewed theoretically as a superposition of multiple vortices according to the PV-based framework (Davis, 1992; Hoskins et al., 1985), as mentioned by Chang (2024). As a practical, ad hoc method, the curvature-based method is effective in determining cyclonic and anticyclonic regions under the effect of shear vorticity, as shown above, and by Okajima et al. (2021) and ONK24. We do not claim that the curvature-based method is the best and only possible way to evaluate cyclonic and anticyclonic contributions to Eulerian eddy statistics. Rather, there are many aspects to be better understood, including the relationship between the relative importance of cyclones/anticyclones and the configuration of the background flow, as discussed by Chang (2024) and shown in Figure 2.

We conclude that the methodology based on local curvature is effective when applied to atmospheric flow fields, either observed or realistically simulated, for evaluating distinct cyclonic and anticyclonic contributions to Eulerian eddy statistics and atmospheric energetics. Results obtained by the methodology are thus physically meaningful and provide insights into the distinct roles of cyclones and anticyclones in storm-track dynamics and eddy-mean flow interactions. Indeed, the crucial importance of the anticyclonic contribution to the midwinter minimum in North Pacific transient eddy activity (Nakamura, 1992; Okajima et al., 2022) obtained by ONK24 is consistent with other studies (Hadas & Kaspi, 2024; Okajima et al., 2023). Our ad hoc method is more feasible in applications to massive data of long-term reanalyzes and climate model outputs. Our framework can apply also to variables such as moisture, precipitation, and turbulent surface heat fluxes (e.g., Okajima, Nakamura, & Spengler, 2024), which are irrelevant to vorticity or PV. Further studies will enrich our insight into the cyclone/anticyclone asymmetry and thereby advance our understanding of atmospheric general circulation.

Data Availability Statement

The JRA-55 reanalysis can be obtained from the Data Integration and Analysis System (DIAS; https://search.diasjp.net/en/dataset/JRA55). The data of the simple cases shown in Figures 1 and 2 is available and archived in Zenodo (Okajima, 2024). Inkscape v1.0.1 (https://inkscape.org/release/1.0.1/) is used to generate the figures.

Acknowledgments
The authors are grateful to the two anonymous reviewers for their sound criticism and valuable comments. We thank E. K. Chang for raising those aspects that have not been explicitly discussed in our earlier works. This study is supported in part by the Japan Society for the Promotion of Science through Grants-in-Aid for Scientific Research 22H01292 and 22K14097, by the Japan Science and Technology Agency through COI-NEXT (JPMJPF2013), and by the Japanese Ministry of Education, Culture, Sports, Science and Technology (MEXT) through the Arctic Challenge for Sustainability II (ArCS-II; JPMXD1420318865).

References

Chang, E. K. (2024). Comment by Chang on "Anticyclonic suppression of the North Pacific transient eddy activity in midwinter". *Geophysical Research Letters*. https://doi.org/10.1029/2024GL110011

Chang, E. K., Lee, S., & Swanson, K. L. (2002). Storm track dynamics. *Journal of Climate*, *15*(16), 2163–2183. https://doi.org/10.1175/1520-0442(2002)015<02163:std>2.0.co;2

Davis, C. A. (1992). Piecewise potential vorticity inversion. *Journal of the Atmospheric Sciences*, *49*(16), 1397–1411. https://doi.org/10.1175/1520-0469(1992)049<1397:ppvi>2.0.co;2

Eyring, V., Gillett, N. P., Achutarao, K., Barimalala, R., Barreiro Parrillo, M., Bellouin, N., et al. (2021). Human influence on the climate system. In V. Masson-Delmotte, P. Zhai, A. Pirani, S. L. Connors, C. Péan, S. Berger, et al. (Eds.) *Climate change 2021: The physical science basis. Contribution of working group I to the sixth assessment report of the intergovernmental panel on climate change* (pp. 423–552). Cambridge University Press.

Hadas, O., & Kaspi, Y. (2024). A Lagrangian perspective on growth of midlatitude storms. *arXiv preprint arXiv:2402.16524*. https://doi.org/10.48550/arXiv.2402.16524

Harada, Y., Kamahori, H., Kobayashi, C., Endo, H., Kobayashi, S., Ota, Y., et al. (2016). The JRA-55 Reanalysis: Representation of atmospheric circulation and climate variability. *Journal of the Meteorological Society of Japanese Series II*, *94*(3), 269–302. https://doi.org/10.2151/jmsj.2016-015

Holton, J. R. (2004). *An introduction to dynamic meteorology* (4th ed.). Academic Press.

Hoskins, B. J., & Hodges, K. I. (2002). New perspectives on the Northern Hemisphere winter storm tracks. *Journal of the Atmospheric Sciences*, *59*(6), 1041–1061. https://doi.org/10.1175/1520-0469(2002)059<1041:npotnh>2.0.co;2

Hoskins, B. J., James, I. N., & White, G. H. (1983). The shape, propagation and mean-flow interaction of large-scale weather systems. *Journal of the Atmospheric Sciences*, *40*(7), 1595–1612. https://doi.org/10.1175/1520-0469(1983)040<1595:tspamf>2.0.co;2

Hoskins, B. J., McIntyre, M. E., & Robertson, A. W. (1985). On the use and significance of isentropic potential vorticity maps. *Quarterly Journal of the Royal Meteorological Society*, *111*(470), 877–946. https://doi.org/10.1256/smsqj.47001

Kobayashi, S., Ota, Y., Harada, Y., Ebita, A., Moriya, M., Onoda, H., et al. (2015). The JRA-55 reanalysis: General specifications and basic characteristics. *Journal of the Meteorological Society of Japanese Series II*, *93*(1), 5–48. https://doi.org/10.2151/jmsj.2015-001

Nakamura, H. (1992). Midwinter suppression of baroclinic wave activity in the Pacific. *Journal of the Atmospheric Sciences*, *49*(17), 1629–1642. https://doi.org/10.1175/1520-0469(1992)049<1629:msobwa>2.0.co;2

Odell, L., Knippertz, P., Pickering, S., Parkes, B., & Roberts, A. (2013). The Braer storm revisited. *Weather*, *68*(4), 105–111. https://doi.org/10.1002/wea.2097

Okajima, S. (2024). Flow fields of simple cases with various configurations of eddies and background flows [Dataset]. *Zenodo*. https://doi.org/10.5281/zenodo.13252873

Okajima, S., Nakamura, H., & Kaspi, Y. (2021). Cyclonic and anticyclonic contributions to atmospheric energetics. *Scientific Reports*, *11*(1), 13202. https://doi.org/10.1038/s41598-021-92548-7

Okajima, S., Nakamura, H., & Kaspi, Y. (2022). Energetics of transient eddies related to the midwinter minimum of the North Pacific storm-track activity. *Journal of Climate*, *35*(4), 1137–1156. https://doi.org/10.1175/jcli-d-21-0123.1

Okajima, S., Nakamura, H., & Kaspi, Y. (2023). Distinct roles of cyclones and anticyclones in setting the midwinter minimum of the North Pacific eddy activity: A Lagrangian perspective. *Journal of Climate*, *36*(14), 4793–4814. https://doi.org/10.1175/jcli-d-22-0474.1

Okajima, S., Nakamura, H., & Kaspi, Y. (2024). Anticyclonic suppression of the North Pacific transient eddy activity in midwinter. *Geophysical Research Letters*, *51*(2), e2023GL106932. https://doi.org/10.1029/2023gl106932

Okajima, S., Nakamura, H., & Spengler, T. (2024). Midlatitude oceanic fronts strengthen the hydrological cycle between cyclones and anticyclones. *Geophysical Research Letters*, *51*(6), e2023GL106187. https://doi.org/10.1029/2023gl106187

Orlanski, I., & Katzfey, J. (1991). The life cycle of a cyclone wave in the Southern Hemisphere. Part I: Eddy energy budget. *Journal of the Atmospheric Sciences*, *48*(17), 1972–1998. https://doi.org/10.1175/1520-0469(1991)048<1972:tlcoac>2.0.co;2

Shaw, T. A., Baldwin, M., Barnes, E. A., Caballero, R., Garfinkel, C. I., Hwang, Y. T., et al. (2016). Storm track processes and the opposing influences of climate change. *Nature Geoscience*, *9*(9), 656–664. https://doi.org/10.1038/ngeo2783

Spensberger, C., Spengler, T., & Li, C. (2017). Upper-tropospheric jet axis detection and application to the boreal winter 2013/14. *Monthly Weather Review*, *145*(6), 2363–2374. https://doi.org/10.1175/mwr-d-16-0467.1

Wallace, J. M., Lim, G. H., & Blackmon, M. L. (1988). Relationship between cyclone tracks, anticyclone tracks and baroclinic waveguides. *Journal of the Atmospheric Sciences*, *45*(3), 439–462. https://doi.org/10.1175/1520-0469(1988)045<0439:rbctat>2.0.co;2